RAPID COMMUNICATIONS

Off-axis spectral beam combining of Bragg reflection waveguide photonic crystal diode lasers

Japanese Journal of Applied Physics **57**, 060312 (2018)
https://doi.org/10.7567/JJAP.57.060312

RAPID COMMUNICATION

Off-axis spectral beam combining of Bragg reflection waveguide photonic crystal diode lasers

Fangyuan Sun[1,2], Lijie Wang[1], Yufei Zhao[1,2], Guanyu Hou[1,2], Shili Shu[1], Jun Zhang[1], Hangyu Peng[1], Sicong Tian[1], Cunzhu Tong[1]*, and Lijun Wang[1]

[1]*State Key Laboratory of Luminescence and Applications, Changchun Institute of Optics, Fine Mechanics and Physics, Chinese Academy of Sciences, Changchun 130033, China*
[2]*University of Chinese Academy of Sciences, Beijing 100049, China*

*E-mail: tongcz@ciomp.ac.cn

Received January 5, 2018; accepted March 29, 2018; published online May 17, 2018

The spectral beam combining (SBC) of Bragg reflection waveguide photonic crystal (BRW-PC) diode lasers was studied for the first time. An off-axis feedback system was constructed using a stripe mirror and a spatial filter to control beam quality in the external cavity. It was found that the BRW-PC diode lasers with a low divergence and a circular beam provided a simplified and cost-effective SBC. The off-axis feedback broke the beam quality limit of a single element, and an M^2 factor of 3.8 times lower than that of a single emitter in the slow axis was demonstrated.

High-power broad-area diode lasers (BALs) are attractive laser sources for numerous applications, such as pumping of fiber lasers, direct material processing, medical treatment, security, and defense.[1)] However, the BALs typically suffer from poor beam quality in the slow axis owing to the multilateral-mode lasing and a large far-field divergence (>30°) in the fast axis caused by the narrow total interface reflection (TIR) waveguide. Several approaches for high-beam-quality BALs have been proposed and beam combining techniques were applied for power scaling.[1–9)] A typical beam combining method is the spectral beam combining (SBC) developed by the Massachusetts Institute of Technology (MIT) Lincoln laboratory,[10,11)] which demonstrated the nearly best beam quality for incoherent combining of diode lasers. However, the beam quality obtained by SBC generally cannot be better than that of a single element.[11–16)] Hence, developing the high-beam-quality single elements and then beam combining have become a route for fabricating high-brightness diode lasers, such as tapered diode lasers and beam combining,[1,17,18)] and slab-coupled optical waveguide lasers (SCOWLs) and beam combining.[2)] Another effort direction is the development of beam combining methods, such as the off-axis feedback.[19–21)]

Bragg reflection waveguide-photonic crystal (BRW-PC) diode lasers[22–24)] and longitudinal photonic bandgap (LPBG) lasers have an intrinsic one-dimensional (1D) photonic bandgap p–i–n structure,[4–6)] with which light is guided by Bragg reflectors with light propagating parallel to epi-layers.[25–28)] The narrow cavity in the vertical direction can be enlarged up to over 10 μm, and a divergence of less than 5° can be realized.[5,6)] A circular laser beam with low divergence was demonstrated,[6)] and the highest continuous wave (CW) emission power reached 12 W.[5)] However, there are only a few investigations on the beam combining of BRW or LPBG BALs, and the advantages of this kind of low-divergence diode lasers for combining are also unclear.

In this study, we investigated the SBC of BRW-PC diode lasers on the basis of an off-axis scheme using an adjustable spatial filter and a stripe refection mirror. The beam quality exceeding that of single elements was realized, which breaks the beam quality limitation of single elements for SBC. These lasers with a low divergence and a circular beam show a highly simplified collimation using a cheap and low-numerical-aperture (NA) aspheric lens. In contrast, cylindrical lenses for fast- and slow-axis collimating are required for the beam combining of conventional BALs. The influence of the position of a spatial filter on the power and beam quality of combined BRW-PC diode lasers was studied.

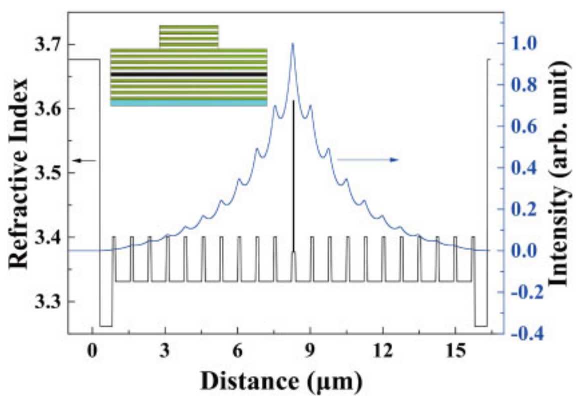

Fig. 1. (Color online) Refractive index and optical field distribution in BRW-PC diode lasers. The inset shows a schematic diagram of a cross section of a BRW-PC diode laser.

Figure 1 shows the refractive index and optical field distribution of the BRW-PC diode lasers, and the inset shows a schematic diagram. A BRW-PC diode laser consists of an optical defect layer, top and bottom Bragg reflectors, which form a 1D photonic bandgap cavity, and only the fundamental transverse mode is allowed.[6)] It is obvious that the fundamental mode is localized with its maximum in the active region and decays away in the Bragg reflectors. The gain medium is composed of two 11 nm $GaAs_{0.86}P_{0.14}$ quantum wells (QWs)[29)] emitting at 808 nm with a 10 nm $Al_{0.4}Ga_{0.6}As$ barrier and embedded in 80 nm $Al_{0.4}Ga_{0.6}As$ optical defect layers. The Bragg reflectors contain 10 periods of $Al_{0.5}Ga_{0.5}As/Al_{0.35}Ga_{0.65}As$ with alternating thicknesses of 600 and 100 nm in the p- and n-sides, respectively, and all interfaces are linearly graded in composition at 20 nm to reduce electrical resistance. The epitaxial layers were grown on a (100)-oriented n+ GaAs substrate by metal–organic chemical vapor deposition (MOCVD), and the devices were fabricated using the standard semiconductor processing techniques. More details can be found in Ref. 6. The laser with a

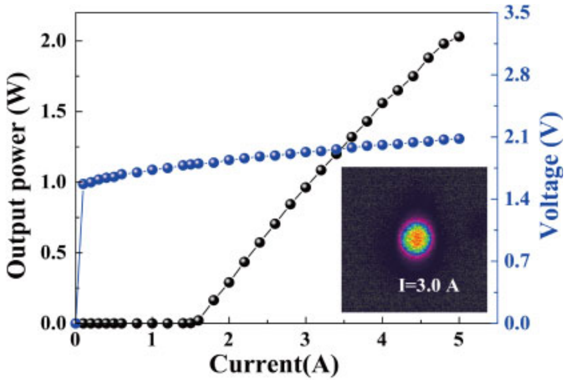

Fig. 2. (Color online) Light–current–voltage characteristics of BRW-PC single emitter. The inset shows the far-field pattern.

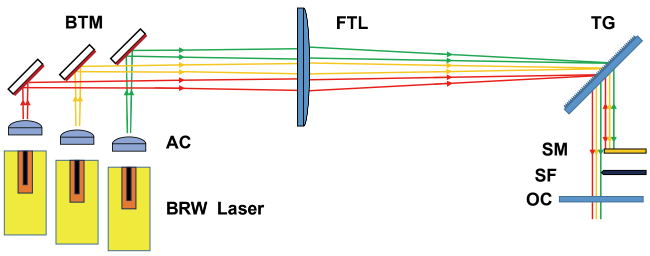

Fig. 3. (Color online) Schematic diagram of SBC setup based on three BRW-PC diode lasers, the off-axis feedback consists of SM and SF. BTM, beam transformation mirror; FTL, Fourier transform lens; TG, transmission grating; AC, aspheric collimator; SM, stripe mirror; SF, spatial filter; OC, output coupler.

low vertical divergence and a circular beam can be realized owing to the large-size optical field in the epitaxy direction.

Figure 2 shows the light–current–voltage (*L*–*I*–*V*) curves of BRW BALs; the inset shows the far-field pattern of a single emitter at 3.0 A and 25 °C. The stripe width is 90 μm and the cavity length is 4 mm. The packaged single emitter with high reflection and antireflection coating yielded approximately 2 W at 5.0 A. The vertical far-field divergence for the definition of full-width at half-maximum (FWHM) is measured to be 7.2°, which corresponds closely to the lateral far-field divergence of 6.9°. The laser beam shows a narrow near-circular emission with an equivalent NA of 0.063 in the fast axis.

Figure 3 shows a schematic diagram of the experimental set up for SBC of three 90 μm BRW-PC single emitters with a cavity length of 4 mm. After aspheric lens collimation (focal length, ∼4.51 mm), the single emitter shows a fast-axis divergence of 0.06° and a slow-axis divergence of 0.91° in $1/e^2$. In contrast, the emitter needs two cylindrical lenses for fast- and slow-axis collimation to obtain similar collimation results for conventional BALs. The BRW BALs with a narrow and circular beam emission provide a low-cost coupling and beam shaping scheme. To stack the beams along the fast-axis direction, the beam transformation mirror (BTM) was designed to transform the directions of the slow and fast axes. A planoconvex Fourier transform lens (FTL) with a focus length of 400 mm was used to extend the beam in the slow axis and overlap the collimated beams of all the BRW-PC single emitters on the Fourier plane, where the transmission grating is positioned. The divergence can be reduced further after FTL; the beam width in the slow axis is about 10 mm. The transmission grating has 1765 lines/mm with a first-order diffraction efficiency of 90% at 808 nm. The incident angle is the Littrow angle of grating, which is about 45.5°. An output coupler (OC) with a reflectivity of 20% was used, and it played an important role in achieving a stable operation of the external cavity despite the relatively weak feedback.

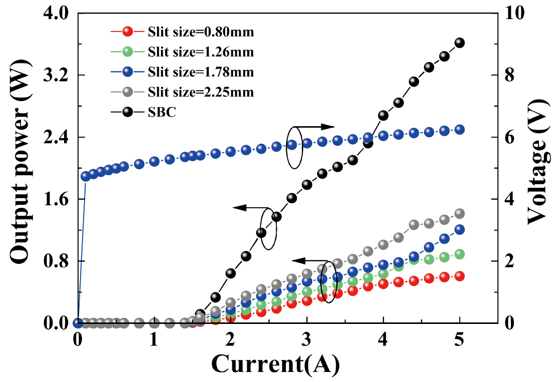

Fig. 4. (Color online) Light–current–voltage characteristics of BRW-PC diode lasers with SBC and off-axis SBC with different slit sizes of spatial filters.

Although the fast-axis divergence has been improved in the BRW-PC diode laser, the lasers still suffer from poor beam quality in the slow axis owing to the intrinsic characteristics of BALs. An off-axis feedback was constructed in the external cavity of SBC via a stripe mirror and a spatial filter to improve the beam quality in the slow axis. The stripe mirror is 2.0 mm wide and coated with a high-reflection dielectric film (>99%). Between the stripe mirror and the OC, an adjustable spatial filter was placed to reduce redundant modes.

The output characteristic of SBC of BRW-PC diode lasers is shown in Fig. 4. Three BRW-PC diode lasers were used and operated at 25 °C. The results of off-axis SBC with different silt sizes of the spatial filter were compared with those of the conventional SBC. It can be seen that the output power over 3.6 W can be realized by SBC. The corresponding slope efficiency is about 1.03 W/A. The application of the off-axis feedback resulted in the decreased output power and slope efficiency. The laser beam width is about 10 mm and the stripe mirror is 2 mm wide, which means that the largest tunable size of the slit is 8 mm. The output powers of BRW-PC diode lasers with off-axis SBC are 0.6, 0.9, 1.2, and 1.4 W at 5.0 A for the slit sizes of 0.80, 1.26, 1.78, and 2.25 mm, respectively. The slope efficiencies are almost proportional to the slit size of the spatial filter, which is because the slit size corresponds to the intensity of the optical feedback. The threshold current of off-axis SBC is 1.4 A and lower than that of conventional SBC.

Although the BRW-PC diode lasers with off-axis SBC showed a decreased output power, this beam quality was improved, which is the intrinsic advantage of off-axis SBC. Figure 5 shows the far-field patterns measured at 40 cm from OC. The far-field pattern of a single emitter after collimation is also shown for comparison. It can be seen that the far-field of SBC is narrow and long. With the decrease in slit size, the beam becomes narrow in the vertical direction or the slow

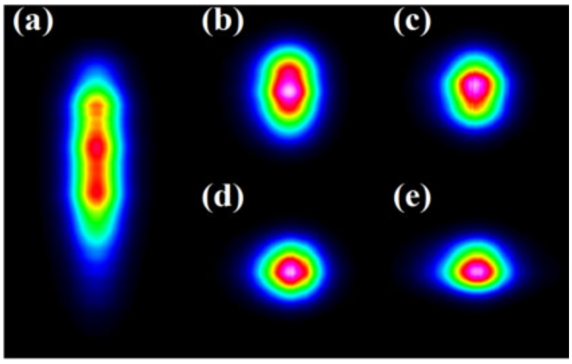

Fig. 5. (Color online) Far-field spots of (a) SBC, off-axis SBC with slit sizes of (b) 2.25, (c) 1.78, (d) 1.26, and (e) 0.8 mm.

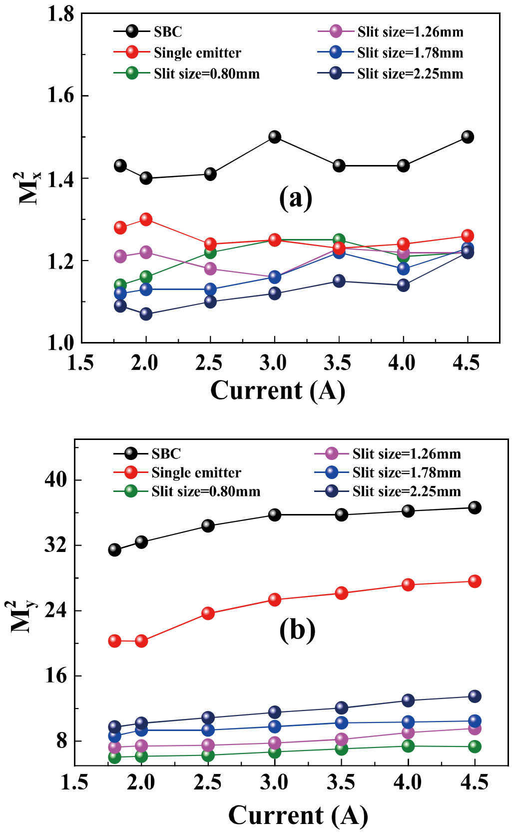

Fig. 6. (Color online) M^2 factors of BRW-PC diode lasers with SBC and off-axis SBC, and single emitter in (a) fast and (b) slow axes.

axis. The far-field spot is nearly circular for a slit size of 1.26 mm.

The beam quality of combined lasers can be described by M^2 factors, which were measured in accordance with ISO11146 and plotted in Fig. 6 as a function of injected current. It can be seen that the laser with SBC shows the worst beam quality, and the beam quality achieved by off-axis SBC exceeds that of the single emitters in both the fast and slow axes. The M^2 factors of the fast axis are shown in Fig. 6(a). For the lasers with SBC, the M^2 factor of the fast axis is approximately 1.45, which is worse than that of the single emitter ($M_x^2 \sim 1.3$) and off-axis SBC. The M^2 factors of the fast axis are 1.07–1.2 for off-axis SBC and slightly improved with the decrease in slit size. With this scheme for the slit size of 2.25 mm, the beam quality is improved from $M_x^2 = 1.25$ for a single emitter to $M_x^2 = 1.12$ at an operation current of 3.0 A.

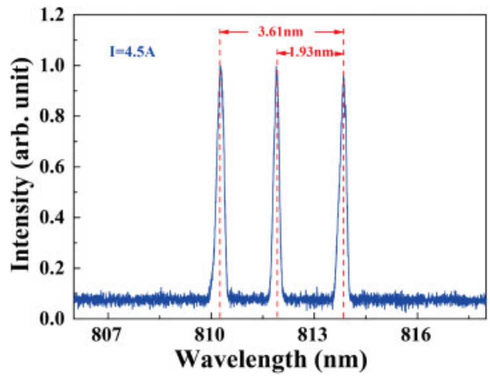

Fig. 7. (Color online) Lasing spectrum of BRW-PC diode lasers with off-axis SBC at 4.5 A.

The M^2 factors of the slow axis are shown in Fig. 6(b). All curves show that the factor increased with the injected current. The typical M^2 factor for SBC is 35.7 at 3.0 A, about 1.4 times as high as that of a single emitter ($M_y^2 = 25.3$). The BRW-PC diode lasers combined using the off-axis scheme show much lower M^2. It is 6.67 at 3.0 A for the combined lasers with a slit size of 0.8 mm, which is improved by a factor of 3.8 compared with the free-running single emitter. For off-axis SBC, the influence of current on beam quality becomes weak with the decrease in slit size. The current dependence coefficient of M_y^2 for a slit size of 2.25 mm is 1.37/A; whereas, it decreases to 0.54/A for a slit size of 0.8 mm. The small slit size indicates a reduced mode number in the slow axis; hence, the far-field blooming induced by the injected current weakens. Although the smaller slit size provides a higher beam quality, the power is also decreased. To clarify the merit of the proposed technique in this work, brightness was calculated according to the definition[30]

$$B = \frac{P}{\lambda^2 M_x^2 M_y^2}, \quad (1)$$

where P is the output power, and λ is the center wavelength. The obtained brightness of off-axis SBC with the slit size of 2.25 mm at 4.5 A is 11.89 MW cm^{-2} sr^{-1}, which reduces to 9.59 MW cm^{-2} sr^{-1} when the slit size is 0.8 mm. In contrast, it is 8.94 MW cm^{-2} sr^{-1} for SBC. Hence, the off-axis SBC improves brightness despite the decreased emission power.

Figure 7 shows the lasing spectrum of BRW-PC diode lasers with off-axis SBC. The spectrum contains three peaks corresponding to three combined single emitters. The wavelength spread is 3.61 nm, and the wavelength spacings of 1.93 and 1.68 nm are observed between two adjacent peaks. The asymmetry of wavelength spacing might be due to the different distances between three adjacent lasers. The wavelength spread $\Delta\lambda$ is related to the focal length of the transform lens (f), the distance between adjacent segments (d), and the dispersion of the grating [$d\alpha/d\lambda = 1/(a\cos\alpha_0)$], where a is the grating period and α_0 is the angle of incidence relative to the grating normal for the center single element. $\Delta\lambda$ can be expressed as $\Delta\lambda = 2da\cos\alpha_0/f$. Generally speaking, the parameters of the grating are accurate, and the influence of the deviation of incident angle α_0 on $\Delta\lambda$ exists but negligible. The main reason is that the realistic adjacent distance deviates from the designed value. In this experiment, α_0 is approximately 45.5° and d is designed to be 2 mm. The calculated wavelength spacing was 1.98 nm, which is in agreement with the measured value of 1.93 nm, and the calculated wavelength spread of 3.96 nm is in agreement with the measured value of 3.61 nm.

In summary, we have studied the SBC of 808 nm BRW-PC diode lasers based on the off-axis feedback system consisting of a stripe mirror and an adjustable spatial filter. The low divergence and circular beam of BRW-PC diode lasers provided a simplified and cost-effective collimation. The application of an off-axis feedback system provided a means of controlling beam quality in the external cavity. The beam quality of the off-axis feedback system exceeding that of the single element was demonstrated and the beam quality can be controlled by the slit size in the spatial filter despite a decrease in emission power. The M^2 factor in the slow axis was improved by about 3.8 times by the off-axis feedback compared with that of the single emitter, and the influence of the injected current was weakened. We believe that these results will contribute to the development of high-power, high-beam-quality BALs.

Acknowledgments We thank the National Natural Science Foundation of China (Nos. 61790584 and 61774153), the International Science Technology Cooperation Program of the Chinese Academy of Sciences (No. 181722-KYSB20160005), Jilin Provincial Natural Science Foundation (No. 20160101243JC), and the Opened Fund of the State Key Laboratory on Integrated Optoelectronics (No. IOSKL2016KF15).

1) M. T. Kelemen, J. Weber, M. Mikulla, and G. Weimann, Proc. SPIE **5723**, 198 (2005).
2) L. J. Missaggia, R. K. Huang, B. Chann, C. T. Harris, J. P. Donnelly, A. Sanchez, and G. W. Turner, Proc. SPIE **6478**, 647806 (2007).
3) T. Wang, C. Z. Tong, L. J. Wang, Y. G. Zeng, S. C. Tian, S. L. Shu, J. Zhang, and L. J. Wang, Appl. Phys. Express **9**, 112102 (2016).
4) I. I. Novikov, N. Yu. Gordeev, Yu. M. Shernyakov, Yu. Yu. Kiselev, M. V. Maximov, P. S. Kop'ev, and A. Sharon, Appl. Phys. Lett. **92**, 103515 (2008).
5) M. J. Miah, V. P. Kalosha, D. Bimberg, J. Pohl, and M. Weyers, Opt. Express **24**, 30514 (2016).
6) L. Wang, C. Tong, S. Tian, S. Shu, Y. Zeng, J. Rong, H. Wu, E. Xing, Y. Ning, and L. Wang, IEEE J. Sel. Top. Quantum Electron. **21**, 1501609 (2015).
7) V. Raab and R. Menzel, Opt. Lett. **27**, 167 (2002).
8) S. G. Strohmaier, G. Erbert, A. H. Meissner-Schenk, M. Lommel, B. Schmidt, T. Kaul, M. Karow, and P. Crump, Proc. SPIE **10086**, 100860C (2017).
9) B. Liu, Y. Liu, and Y. Braiman, Opt. Express **18**, 7361 (2010).
10) V. Daneu, A. Sanchez, T. Y. Fan, H. K. Choi, G. W. Turner, and C. C. Cook, Opt. Lett. **25**, 405 (2000).
11) R. K. Huang, B. Chann, L. J. Missaggia, J. P. Donnelly, C. T. Harris, G. W. Turner, A. K. Goyal, T. Y. Fan, and A. Sanchez-Rubio, IEEE Photonics Technol. Lett. **19**, 209 (2007).
12) T. Y. Fan, IEEE J. Sel. Top. Quantum Electron. **11**, 567 (2005).
13) Z. Zhu, L. Gou, M. H. Jiang, Y. L. Hui, H. Lei, and Q. Li, Opt. Express **22**, 17804 (2014).
14) H. Meng, X. Ruan, Z. Wang, W. Du, L. Guo, H. Tan, S. Gao, and D. Wu, IEEE Photonics J. **9**, 1501506 (2017).
15) H. C. Meng, T. Y. Sun, H. Tan, J. H. Yu, W. C. Du, F. Tian, J. M. Li, S. X. Gao, X. J. Wang, and D. Y. Wu, Opt. Express **23**, 21819 (2015).
16) J. Zhang, H. Y. Peng, X. H. Fu, Y. Liu, L. Qin, G. Q. Miao, and L. J. Wang, Opt. Express **21**, 3627 (2013).
17) D. Vijayakumar, O. B. Jensen, R. Ostendorf, T. Westphalen, and B. Thestrup, Opt. Express **18**, 893 (2010).
18) A. Müller, D. Vijayakumar, O. B. Jensen, K. Hasler, B. Sumpf, G. Erbert, P. E. Andersen, and P. M. Petersen, Opt. Express **19**, 1228 (2011).
19) D. Vijayakumar, O. B. Jensen, and B. Thestrup, Opt. Express **17**, 5684 (2009).
20) O. B. Jensen, B. Thestrup, P. E. Andersen, and P. M. Petersen, Appl. Phys. B **83**, 225 (2006).
21) A. Jechow, V. Raab, and R. Menzel, Appl. Opt. **45**, 3545 (2006).
22) A. Jechow, M. Lichtner, R. Menzel, M. Radziunas, D. Skoczowsky, and A. G. Vladimirov, Opt. Express **17**, 19599 (2009).
23) S. Nojima, Jpn. J. Appl. Phys. **38**, L867 (1999).
24) R. Nakao and M. Morifuji, Jpn. J. Appl. Phys. **52**, 012002 (2013).
25) V. N. Konopsky, E. V. Alieva, S. Y. Alyatkin, A. A. Melnikov, S. V. Chekalin, and V. M. Agranovich, Light: Sci. Appl. **5**, e16168 (2016).
26) B. J. Bijlani and A. S. Helmy, Opt. Lett. **34**, 3734 (2009).
27) C. Z. Tong, B. Bijlani, S. Alali, and A. S. Helmy, IEEE J. Quantum Electron. **46**, 1605 (2010).
28) L. J. Wang, Y. Yang, Y. G. Zeng, L. J. Wang, C. Z. Tong, X. N. Shan, H. X. Zhao, R. Wang, and S. F. Yoon, Appl. Phys. B **107**, 809 (2012).
29) X. Li, H. Wang, Z. L. Qiao, Y. P. Liao, Y. Zhang, Y. Q. Xu, Z. C. Niu, C. Z. Tong, and C. Y. Liu, Jpn. J. Appl. Phys. **56**, 050310 (2017).
30) R. Diehl, *High-Power Diode Lasers Fundamentals Technology Applications* (Springer, Heidelberg, 2000) p. 56.